Reversible switching characteristics of polyfluorene-derivative single layer film for nonvolatile memory devices

Tae-Wook Kim, Seung-Hwan Oh, Hyejung Choi, Gunuk Wang, Hyunsang Hwang, Dong-Yu Kim, and Takhee Lee[a)]
Heeger Center for Advanced Materials, Department of Materials Science and Engineering, Gwangju Institute of Science and Technology, Gwangju 500-712, Republic of Korea

(Received 27 February 2008; accepted 9 June 2008; published online 27 June 2008)

This letter reports on reversible switching behavior of metal-insulator-metal type nonvolatile organic memory devices using polyfluorene-derivative (WPF-oxy-F) single layer film. The current-voltage (*I-V*) characteristics showed that the WPF-oxy-F single layer film has two distinguished resistance states, low resistance state and high resistance state, with four orders of on/off ratio ($I_{on}/I_{off} \sim 10^4$). From the analysis of *I-V* curves, area dependent *I-V* characteristics, and current images obtained by conducting atomic force microscopy we propose that the space charge limited current with filamentary conduction is a potential mechanism for the reversible switching behavior of WPF-Oxy-F memory devices. © *2008 American Institute of Physics*.
[DOI: 10.1063/1.2952825]

Recently, organic nonvolatile memory appears highly attractive, owing to its potential application in data storage.[1–10] Many efforts have been made to realize organic bistable memory devices exhibiting nonvolatile memory with two different states of resistivity, i.e., a high resistance state (HRS) and a low resistance state (LRS).[1–10] Polyfluorene derivatives which are conjugated polymer for organic devices are one of the candidates to satisfy the essential conditions for high performance non volatile memory devices,[4–6] owing to their native properties such as good processability and endurance against oxidation.[11] Recent reports on the electrical bistability in polyfluorene-based organic materials have showed relevant performances for nonvolatile memory applications.[4–6,12] However, specific electrical characteristics of polyfluorene-based organic memory devices is still necessary to understand the origin of reversible switching behavior.

In this letter, we report on the reversible switching behavior of polyfluorene-derivative (WPF-oxy-F) single layer film. From analysis on the current-voltage (I-V) characteristics on the log-log scale and the current images of the two different resistance states by conducting atomic force microscopy (CAFM), a mechanism for the reversible switching of the WPF-oxy-F memory devices is proposed.

The polyfluorene-derivative (WPF-oxy-F), schematically shown in Fig. 1(a), was synthesized by a palladium catalyzed Suzuki coupling reaction method.[13] The metal-insulator-metal (MIM) type polyfluorene-derivative memory devices were fabricated on a heavily doped *p*-type (100) silicon (p^+ Si)substrate (0.001–0.015 Ω cm). After the typical ultrasonic cleaning processes with acetone, methanol, and deionized water, silicon wafer was treated via a diluted HF-last process to remove the native oxide layer. WPF-oxy-F was first dissolved in methanol at a concentration of 5 mg/ml, and then was spin coated on the substrate. The typical spin-coating condition was 2000 rpm for 30 s, and the resulting thickness of the film was measured to be around 30 nm. Postbaking was performed at 150 °C for 20 min on a hotplate in a nitrogen-filled glovebox. The top electrodes were patterned with a shadow mask that had square patterns of four different areas: 50×50, 100×100, 200×200, and 400×400 μm^2. A 100 nm thick Ag layer was deposited as the top electrode using a thermal evaporator under a pressure of 10^{-6} Torr. A memory device structure is schematically shown in Fig. 1(b). The current-voltage (*I-V*) measurements were carried out using a semiconductor parameter analyzer (Agilent Technology B1500A).

Figure 2 shows a representative *I-V* characteristic of a single layer Ag/WPF-oxy-F/p^+ Si memory device with a junction area of 50×50 μm^2. When we applied the positive bias from 0 to 5 V to the Ag top electrode, the current increased gradually with the applied bias (stage 1). Then, a sharp increase in current was observed near a transition voltage at ~4 V, indicating the transition of the organic memory device from a HRS to a LRS. To prevent the electrical breakdown of the device, a current compliance was set to 1 mA. After the transition from a HRS to a LRS, the device remained in the LRS during the voltage sweep in the negative bias direction from 5 to 0 V (stage 2). A semilog plot of this *I-V* characteristic (inset of Fig. 2) clearly shows the electrical bistability of WPF-oxy-F with a high on/off ratio (e.g., $I_{on}/I_{off} \sim 10^4$ at 0.3 V). Although most measurement was performed under ambient condition, any noticeable degradation of switching behavior was not observed compared to the results measured under inert gas condition, as shown in inset of Fig. 2. When the bias was swept continuously in the negative bias direction from 0 to −3 V (stage 3), the current decreased, implying another transition of the memory device from LRS to HRS. After this stage, the device showed a

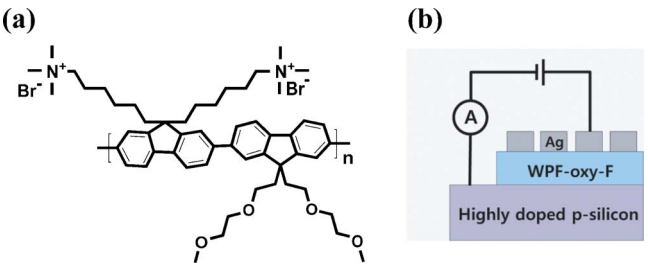

FIG. 1. (Color online) (a) Chemical structure of WPF-oxy-F polyfluorene derivative. (b) Schematic of single component WPF-oxy-F memory device.

[a)]Electronic mail: tlee@gist.ac.kr.

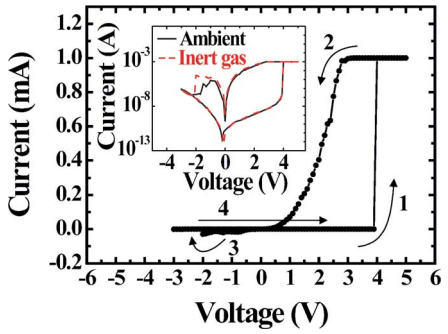

FIG. 2. (Color online) *I-V* characteristics of a WPF-oxy-F memory device. Inset shows the semilog plot of the *I-V* characteristics measured in ambient (black solid line) and inert gas condition (red dash line).

pristine HRS (stage 4). When the bias was applied in the positive bias direction repeatedly, the device showed almost identical *I-V* characteristics at the range between −3 and 5 V, indicating the reversible switching behavior.

To understand the origin of switching behavior of WPF-oxy-F, we performed further analysis on WPF-oxy-F memory devices. The inset in Fig. 3(a) shows the energy band diagram of the Ag/WPF-oxy-F/p^+ Si device. Consideration of the work functions of Ag (4.3 eV) and p^+ Si (5.17 eV) reveals that the Ag top contact on WPF-oxy-F acts as a very high barrier for the electron transport, whereas the p^+ Si contact is efficient for hole injection into the WPF-oxy-F layer.

In general, *I-V* curves have been analyzed to study the mechanism underlying bistable switching in memory devices.[10,14] For example, by investigating the current-voltage relationships of *I-V* curves on the log-log scale, space charge limited current[15–17] (SCLC) or filamentary conductions[18–20] has been suggested as a potential mechanism for charge transport in organic devices. Figure 3(a) shows a log-log plot of the *I-V* curve in the positive bias region for a WPF-oxy-F memory device. This figure shows four distinct regimes, which is similar to previously reported results for some organic devices.[16,17] As shown in Fig. 3(a), at a low bias region or Ohmic regime (1), the current is linearly proportional to the voltage as a result of the thermally generated free carriers.[15–17] In this regime, the current density J can be described as

$$J = \frac{qn_0\mu V}{d}, \tag{1}$$

where n_0 is the density of free carriers, d is the thickness of the polymer layer, and μ is the carrier mobility. At an intermediate bias region or SCLC trap-limited regime (2), the current is controlled by the traps in the polymer layer via thermally activated hopping conduction.[15–17] In this regime, the current obeys the Mott–Gurney law as

$$J = \frac{9\varepsilon\varepsilon_0\mu\Theta V^2}{d^3}, \tag{2}$$

where Θ is the trapping fraction, ε is the dielectric constant of the polymer, and ε_0 is the permittivity of free space.[15–17] When the voltage is increased further, the traps in the polymer film will be almost filled. This region is described as trap-filled limit regime (3), in which the current flows via thermionic emission and a Fowler–Nordheim conduction mechanism, so that the current increases sharply and the device changes from HRS to LRS.[16] From the single-carrier SCLC conduction theory,[17] the trap density (N_t) in the polymer layer can be explained in terms of a voltage (V_{TFL}) required to fill the traps in the polymer layer and is expressed as

$$N_t = \frac{3\varepsilon\varepsilon_0 V_{\mathrm{TFL}}}{2qd^2}, \tag{3}$$

where q is the electronic charge. After transition from HRS to LRS, most of the trap sites in the polymer film are filled and the current flow is free from the influence of traps in the polymer film. This region is called a trap-free SCLC regime (4), and the *I-V* curve fits very well with $I \propto V^2$.[15–17] Based on the analysis of the log-log plot of the *I-V* curves [Fig. 3(a)], the reversible switching behavior of the WPF-oxy-F memory devices is due to the transition between the trap-limited SCLC and the trap-free SCLC.

Although the conduction mechanism of WPF-oxy-F can be well explained by trap-limited and trap-free SCLC processes, the abrupt jump of current by almost four orders of magnitude is not normal in SCLC conduction.[21] It seems that additional effect such as filamentary conduction might affect the switching behavior of WPF-oxy-F memory devices as well. Recent reports on switching mechanism of organic memory device well explained the formation of metallic filamentary due to the migration of metal ions from the top electrodes such as silver and copper.[19,20] The switching behavior of such organic memory devices based on filamentary conduction is significantly affected by the threshold voltage which is the minimum bias for ionization and migration of metallic electrode.[20] The switching behavior was investigated by varying the program voltage conditions, as summarized in Fig. 3(b). Here, the voltage sweep back and forth was made from −2.5 V (starting voltage) to 3, 3.5, 4, 4.5, and 5 V (program voltages; marked with arrows), as shown in the inset of Fig. 3(b). The current values at each *I-V* curve with different program voltages were measured at 0.3 V (read voltage). When the program voltage was less than 4.0 V, the memory device did not switch and there was no difference between HRS and LRS with very similar current level (~10 pA). On the other hand, when the program voltage was larger than 4.0 V, the device started to exhibit

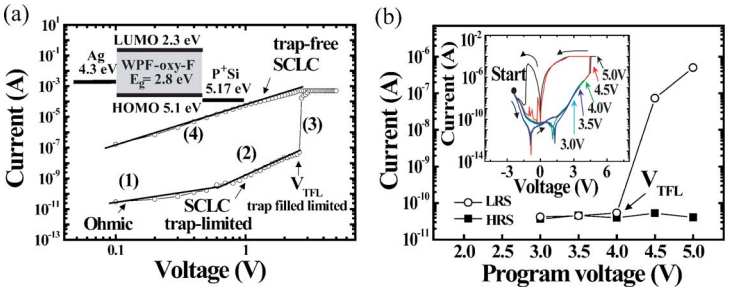

FIG. 3. (Color online) (a) *I-V* characteristics of a WPF-oxy-F memory device in log-log scale. Inset figure shows energy band diagram of WPF-oxy-F memory device. (b) Programming voltage dependence of a WPF-oxy-F memory device. Excess bias (V_{th}) required changing the resistance of WPF-oxy-F memory device from HRS to LRS. The inset figure shows stop voltage dependent *I-V* characteristic.

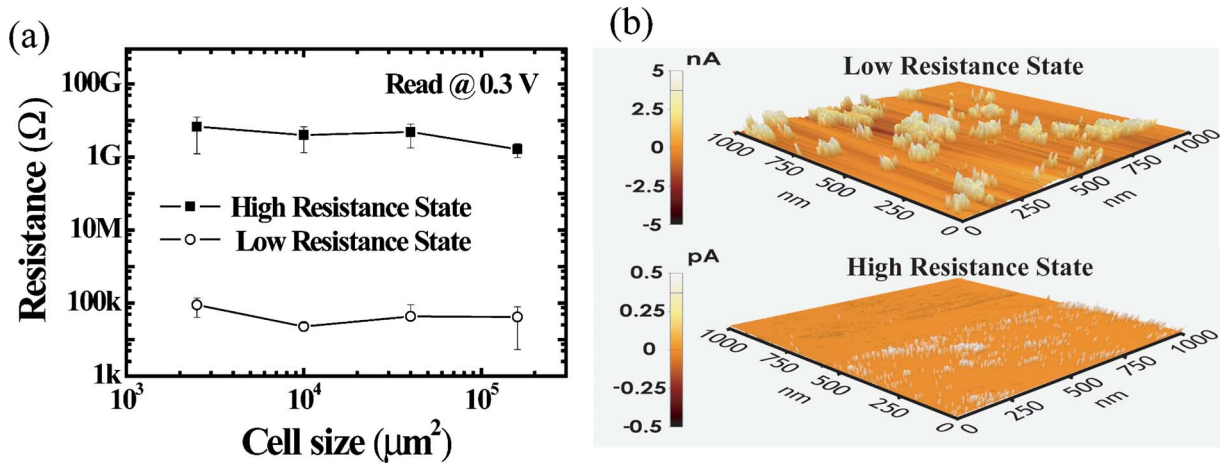

FIG. 4. (Color online) (a) Resistance values of two resistance states (HRS and LRS) of a WPF-oxy-F memory device as a function of the junction areas. (b) Current images of high and LRSs obtained by CAFM measurement.

switching behavior and LRS showed a current higher than ~100 nA, while HRS remained in ~10 pA current level. In this voltage range, the device clearly showed reversible switching behavior, requiring the threshold voltage (V_{th}) to fill the traps and form the metallic filament in the polymer layer. However, since the more traps are occupied the higher current flows, therefore trap-filling process may create high-current paths which in turn may lead to electromigration and filamentary conduction paths.

Figure 4(a) shows a summary of the resistance states of the WPF-oxy-F devices (~100 devices) measured at different areas. From this figure, one can see that LRS did not change with the variation of the junction area; instead, the resistance remained about 100 kΩ. In contrast, the resistance value of the HRS slightly decreased from 6.8 to 1.6 GΩ as the junction area increased. To investigate this observation, we examined the current images of HRS and LRS acquired with CAFM. Figure 4(b) shows each current image for HRS and LRS of a WPF-oxy-F layer on p^+ Si without a top Ag electrode. An Ag-coated AFM tip was first scanned over the memory junction area under a voltage of 6.5 V applied to the CAFM tip relative to a WPF-oxy-F/p^+ Si sample (programming process). Then, the current image of LRS was obtained under a 1.0 V tip bias condition (reading process). Similarly, the current image of HRS was obtained at a 1.0 V tip bias after the CAFM tip was scanned over the junction area under a −3.0 V tip bias (erasing process). As can be seen in these images, the current level of the HRS is uniformly very small (typically less than ~0.5 pA). On the contrary, there are localized and distributed conduction paths in the current image of the LRS (typically ~4 nA). Due to the different measurement conditions such as contact area and tip probing condition, the current levels of the HRS and LRS measured by CAFM were relatively lower than those measured in the MIM type devices. However, The on/off ratio in the current images was still about 10^3, indicating good reversible switching characteristics. This result suggests that switching behavior does not occur uniformly over the junction area. Instead, the localized current paths in LRS explain the reversible switching of WPF-oxy-F memory devices.

In conclusion, organic memory devices were fabricated using single component polyfluorene-derivative (WPF-oxy-F) as MIM-type device structures. The memory devices showed excellent reversible switching performance for non-volatile memory devices, such as a large on/off (I_{on}/I_{off}) ratio of more than 10^4. From the *I-V* characteristics and current images, the SCLC with filamentary conduction contributes to the switching behavior of WPF-Oxy-F memory device.

This work was supported by the National Research Laboratory (NRL) Programs of the Korea Science and Engineering Foundation (KOSEF), the Program for Integrated Molecular System at GIST, and SystemIC2010 project of Korea Ministry of Knowledge Economy.

[1] L. D. Bozano, B. W. Kean, V. R. Deine, J. R. Salem, and J. C. Scott, Appl. Phys. Lett. **84**, 607 (2004).
[2] Q. Ling, Y. Song, S. J. Ding, C. Zhu, D. S. H. Chan, D.-L. Kwong, E.-T. Kang, and K.-G. Neoh, Adv. Mater. (Weinheim, Ger.) **17**, 455 (2005).
[3] R. J. Tseng, C. O. Baker, B. Shedd, J. Huang, R. B. Kaner, J. Ouyang, and Y. Yang, Appl. Phys. Lett. **90**, 531011 (2007).
[4] C. Pearson, J. H. Ahn, M. F. Mabrook, D. A. Zeze, M. C. Petty, K. T. Kamtekar, C. Wang, M. R. Bryce, P. Dimitrakis, and D. Tsoukalas, Appl. Phys. Lett. **91**, 123506 (2007).
[5] Q.-D. Ling, E.-T. Kang, K.-G. Neoh, Y. Chen, X.-D. Zhuang, C. Zhu, and D. S. H. Chan, Appl. Phys. Lett. **92**, 143302 (2008).
[6] T.-W. Kim, S.-H. Oh, H. Choi, G. Wang, H. Hwang, D.-Y. Kim, and T. Lee, "Reliable Organic Nonvolatile Memory Device Using a Polyfluorene-Derivative Single-Layer Film," IEEE Electron Device Lett. (in press).
[7] Y. Yang, L. Ma, and J. Wu, MRS Bull. **29**, 833 (2004).
[8] J. C. Scott and L. D. Bozano, Adv. Mater. (Weinheim, Ger.) **19**, 1452 (2007).
[9] M. Karakawa, M. Chikamatsu, Y. Yoshida, R. Azumi, K. Yase, and C. Nakamoto, Macromol. Rapid Commun. **28**, 1479 (2007).
[10] C.-H. Tu, Y.-S. Lai, and D.-L. Kwong, IEEE Electron Device Lett. **27**, 354 (2006).
[11] U. Scherf and E. J. W. List, Adv. Mater. (Weinheim, Ger.) **14**, 477 (2002).
[12] T. Ouisse and O. Stéphan, Org. Electron. **5**, 251 (2004).
[13] S.-H. Oh, S.-I. Na, Y.-C. Nah, D. Vak, S.-S. Kim, and D.-Y. Kim, Org. Electron. **8**, 773 (2007).
[14] J. Chen, L. Xu, J. Lin, Y. Geng, L. Wang, and D. Ma, Appl. Phys. Lett. **89**, 083514 (2006).
[15] M. A. Lampert and P. Mark, *Current Injection in Solids* (Academic, New York, 1970), p. 59.
[16] H.-T. Lin, Z. Pei, and Y.-J. Chan, IEEE Electron Device Lett. **28**, 569 (2007).
[17] M. Arif, M. Yun, S. Gangopadhyay, K. Ghosh, L. Fadiga, F. Galbrecht, U. Scherf, and S. Guha, Phys. Rev. B **75**, 195202 (2007).
[18] G. Dearnaley, D. V. Morgan, and A. M. Stoneham, J. Non-Cryst. Solids **4**, 593 (1970).
[19] S. Ssenyange, H. Yan, and R. L. McCreery, Langmuir **22**, 10689 (2006).
[20] W.-J. Joo, T.-L. Choi, K.-H. Lee, and Y. Chung, J. Phys. Chem. B **111**, 7756 (2007).
[21] A. Carbone, B. K. Kotowska, and D. Kotowski, Phys. Rev. Lett. **95**, 236601 (2005).